

# Different Zeolite Phases Obtained with the Same Organic Structure Directing Agent in the Presence and Absence of Aluminum: The Directing Role of Aluminum in the Synthesis of Zeolites

Omer F. Altundal, Santiago Leon, and German Sastre\*



Cite This: *J. Phys. Chem. C* 2023, 127, 10797–10805



Read Online

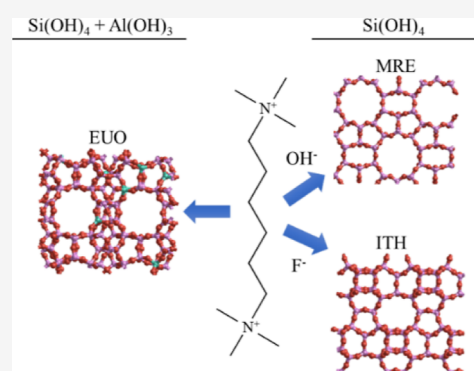
ACCESS |

Metrics & More

Article Recommendations

Supporting Information

**ABSTRACT:** Zeolites are a large family of crystalline microporous materials with, mainly, silicate and aluminosilicate composition. Each topology can only be synthesized in a specific range of aluminum content, Al/(Si + Al), within the interval [0–0.5], and this interval cannot, in general, be predicted for each structure. Aluminum and organic structure directing agents (OSDAs), among others, act together in obtaining the zeolite phase under each specific synthesis condition. The present study is an attempt to rationalize the role of aluminum as a structure directing agent in the synthesis of zeolites using computational chemistry and based on the criteria of energetic stability using both force field and periodic DFT methods. A proper selection of cases in which, using the same OSDA, different zeolite phases are obtained in the presence and absence of aluminum helps to rationalize how aluminum contributes to the relative stability of the different competing zeolite phases considered.



## 1. INTRODUCTION

Zeolites are nowadays a large family of crystalline microporous materials made of corner-sharing  $\text{TO}_{4/2}$  tetrahedra, with T being an atom with tetrahedral coordination such as—mainly—Si, B, Al, Ge, and P. The composition of zeolites can be expressed as  $\text{OSDA}^{m+}_b \text{M}^{n+}_a \text{Al}_x \text{P}_y \text{Si}_{1-x-y} \text{O}_2$ , with the electroneutrality condition  $x = n \cdot a + m \cdot b + y$ . Trivalent atoms other than Al are allowed, such as B, Ga, Be, and very rarely N; tetravalent atoms are typically Si and Ge; and pentavalent atoms are—when present—almost exclusively P and very rarely As. Also, framework atoms can be divalent, such as Zn and Mg. Extra framework cations, hence located in the micropore, are  $\text{M}^{n+}$  (inorganic) and  $\text{OSDA}^{m+}$  (organic), which are incorporated during the synthesis and play the role of a structure directing agent (SDA). Exceptionally, protons are the only cations located in the framework, forming Brønsted acid sites such as  $\equiv\text{Si}(\text{H})\text{Al}\equiv$ .

Since their discovery (stilbite) as minerals in 1752 by Axel F. Cronstedt, a large majority of known (ca. 67) natural zeolites are aluminosilicates, but synthesis in the laboratory allowed us to expand vastly the chemical composition as outlined above and also the number of topologies found. Although aluminosilicate is still the preferred chemical composition for catalytic applications, the name zeolite can be applied to all chemical compositions compatible with the microporous corner-sharing tetrahedra coordination that defines the family. However, the full definition also requires some conditions for an appropriate structural characterization, which is sometimes precluded due to the presence of intergrowths. Hence, if the

sample does not contain a sufficient amount of end polymorph, it will be provisionally excluded from the database of zeolite structures and will be moved to the database of disordered zeolite structures. This separation has been formally introduced very recently. At the time of this update, the number of zeolites moved from the first group (ordered) to the second (disordered) was 7 (BEA, CTH, MRE, PCS, SFV, STO, and UOE), and the number of “Zeolite Structures” decreased from 253 to 246. Finally, in an extension of the above concepts, interrupted structures (those containing terminal  $\equiv\text{Si}-\text{O}$ ) are also accepted as zeolites. Currently, there are 14 interrupted zeolite frameworks described: -CHI, -CLO, -EWT, -IFT, -IFU, -IRY, -ITV, -LIT, -PAR, -RON, -SSO, -SVR, -SYT, and -WEN.

The structural characterization does not imply that the atomic positions are chemically ordered, and so in zeolites, it is very usual to achieve a structural characterization without full knowledge of the chemical distribution of atoms, and so in particular, for aluminosilicates, the aluminum distribution is not known in full detail.  $^{29}\text{Si}$  and  $^{27}\text{Al}$  MAS NMR allow us to reduce the number of possibilities so that, among all possibilities, only those meeting certain criteria are compatible with the characterization.<sup>1–5</sup>

Received: March 7, 2023

Revised: April 19, 2023

Published: May 30, 2023



Different synthesis conditions have been described so that, with the same Si/Al ratio in the same zeolite, several possibilities of Al ordering are generated, and they can show notable differences in specific catalytic applications. Li et al.<sup>6</sup> introduced B atoms to the synthesis of ZSM-5 structures to direct the Al atoms to 10-rings channels which enhanced the catalytic activity of ZSM-5 samples for hexene cracking. While investigating the methanol-to-dimethyl ether (DME) reaction by density functional theory (DFT) calculations, Ghorbanpour et al.<sup>7</sup> found that Al atoms in different T sites of H-ZSM-5 alter the Gibbs free energy profile of the reaction. Biligetü et al.<sup>8</sup> utilized various straight- and branched-chain alcohols in the synthesis gel to observe their effect on the Al distribution and the catalytic performance of ZSM-5 zeolite. They concluded that ZSM-5 synthesized with trimethylolethane in combination with Na cations in the synthesis gel had the best catalytic activity for methanol-to-olefin reaction due to Al atoms being preferentially siting in 10-ring channels. Chu et al.<sup>9</sup> synthesized FER-type zeolites using various linear and cyclic organic structure directing agents (OSDAs) under fluoride and hydroxide medium to elucidate the relationship between Al locations in FER-type zeolites and their catalytic activity in DME carbonylation reaction. They found out that FER-type zeolites are not ideal catalysts for DME carbonylation reaction due to their Al atoms being mostly constrained on T1 and T3 sites which are inactive for the reaction, regardless of the OSDA or the synthesis media. Vjunov et al.<sup>10</sup> analyzed the Al distribution HBEA zeolite with different Si/Al contents using DFT-generated extended X-ray absorption fine structure spectra of the structures. Their results showed that the Al atoms in the crystallographic sites T-7 and T-2 are more susceptible to be removed as the Al content of the structure decreases. Perea et al.<sup>11</sup> used atom probe tomography to determine the location and nearest Al neighbors of framework Al atoms in ZSM-5. They discovered that the Al atoms, which are normally distributed uniformly in ZSM-5 with a probable Al–Al neighbor distance of  $18 \pm 6 \text{ \AA}$ , start forming clusters after severe steam-treating of the structure (a probable Al–Al neighbor distance of  $9 \pm 3 \text{ \AA}$ ). These works, along with many others,<sup>12–21</sup> show the importance of Al location of the catalytic performance of zeolites.

Early studies by Shantz and co-workers<sup>22–24</sup> used <sup>29</sup>Si and <sup>27</sup>Al NMR to study the aluminum distribution of Al-ZSM-12 zeolite and found that rather than random it is controlled by the OSDA used in the synthesis. The Al atoms (+3 formal charge) behave as pseudo-negative charges compared to Si atoms (+4) and tend to locate close to the positive charge of the OSDA molecule. A similar result was found when Li et al.<sup>25</sup> studied the effect of *N,N,N*-trimethyl-1-adamantyl ammonium on the Al distribution in SSZ-13. In this way, the OSDA has not only the effect of directing the synthesis toward a particular structure but is also responsible for the Al distribution in the as-made zeolite. Also, in the case of ZSM-18, the OSDA (tris-methyl-pyrrolidinium) does not only stabilize the structure but also drives the Al location almost exclusively to the T3 (3-rings) crystallographic position.<sup>26</sup> The directing role of OSDAs in the synthesis of zeolites has been widely explored in the literature.<sup>27–38</sup>

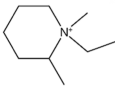
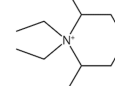
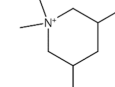
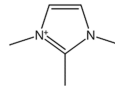
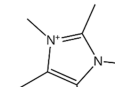
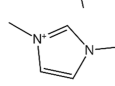
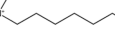
While the conceptual idea on the role of an OSDA in Al distribution is simple, a more difficult challenge is to unveil the role of Al in driving the synthesis toward a specific zeolite phase. The most general question is how do we guess the zeolite obtained using as input the synthesis conditions? This

question is of course the holy grail of the synthesis of zeolites, and we are still far from having a general explanation, although undoubtedly a considerable advance has been done in the last 70 years, with excellent reviews available in the literature.<sup>29,39,40</sup> The aim of this study is not so general, and thus, a relatively simple strategy has been devised in order to unveil how Al drives the synthesis to specific zeolites. For this task, pairs of synthesis routes have been selected so that they (a) employ the same OSDA and (b) give different phases when using pure silica and aluminosilicate gels. In this way, we can conclude that if the absence/presence of Al gives different zeolites, with—roughly—all other synthesis parameters being the same, then the role of Al, when present, is a crucial factor to explain the zeolite phase obtained. Further, the use of computational methods does not only allow us to compare the total energies and establish if the zeolite obtained is driven thermodynamically, as that with lowest energy, but also should allow us to calculate the different contributions to the energy and analyze which of them play a more dominant role in order to justify the phase obtained. Similar ideas have been recently used to computationally analyze the role of fluoride, by comparing synthesis routes that give different pure silica zeolites using the same OSDA in the absence/presence of fluoride.<sup>41</sup> Among other results, this study suggests an explanation regarding the competition of pure silica UFI vs LTA when using 1,2-dimethyl-3-(2-fluorobenzyl)imidazolium as an OSDA forming self-assembling dimers in the *lta* cavities present in both zeolites. The presence of the additional [4<sup>5</sup>5<sup>4</sup>6<sup>4</sup>8] cavities in UFI allows a larger relaxation of the *lta* cavities, considerably strained by the presence of OSDA dimers, hence giving UFI in OH<sup>−</sup> media. In fluoride media, the more compact electrostatic packing of SDA<sup>+</sup>-F<sup>−</sup> in LTA, without the [4<sup>5</sup>5<sup>4</sup>6<sup>4</sup>8] cavities of UFI, contributes to a larger electrostatic stabilization, giving LTA as a product. In a similar way, the present study intends to guess general rules about aluminum incorporation in zeolites that may ultimately lead to understand and predict the most probable Si/Al interval upon which each zeolite can be synthesized.

## 2. COMPUTATIONAL METHODS

**2.1. OSDA Search Details.** In this article, as well as in our recent previous study,<sup>41</sup> we introduce the idea of “competing phases” from a strict experimental viewpoint. As a consequence, the list of “competing zeolites” is obtained from all zeolites experimentally synthesized with a given OSDA, either as pure silica or as aluminosilicate. Unlike previous works in which, for each OSDA, all known zeolites were calculated with the aim of searching new OSDAs for the synthesis of zeolites,<sup>42,43</sup> the aim of the present work is rather trying to explore the experimental interval of chemical composition with which certain zeolites can be obtained. To achieve this, an exhaustive literature search was performed using SciFinder.<sup>44</sup> Specific keywords were introduced in the “reference search” in order to find OSDAs, and a total of 8754 publications + patents were identified, each of the records containing an extended information including the abstract. An algorithm was designed in order to remove records corresponding to (a) germanium-containing zeolites; (b) MFI, FAU, and MOR as the material names of the zeolite structure since these structures can be easily synthesized without an OSDA; (c) zeolites synthesized in the presence of inorganic cations (e.g., Na<sup>+</sup> and K<sup>+</sup>); (d) zeolites synthesized in the presence of seed crystals; and (e) patents since they

**Table 1.** Names and Structures of the Seven OSDA Molecules and the Zeolite Phases That Are Obtained by Using Them under Pure Silica and Aluminosilicate Conditions

OSDA	Name	Pure-Silica	Aluminosilicate	Structure
SDA1	1-ethyl-1,2-dimethylpiperidinium	BEA, SGT, DDR, DOH	CHA, MTW	
SDA2	1,1-diethyl-2,6-dimethylpiperidinium	SFF	AEI, SFF	
SDA3	1,1,3,5-tetramethylpiperidinium	MTW	AEI, CHA	
SDA4	1,2,3-trimethylimidazolium	ITW	RTH	
SDA5	1,2,3,4,5-pentamethylimidazolium	STW	RTH	
SDA6	1,3-dimethylimidazolium	ITW, TON	FER	
SDA7	hexamethonium	ITH, MRE	EUO	

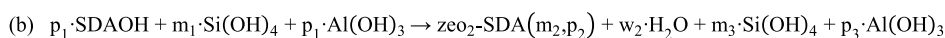
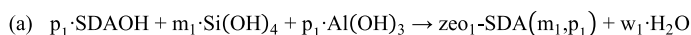
rarely disclose all relevant information regarding the synthesis procedure. For instance, in the study by Dusselier et al.,<sup>45</sup> the authors synthesized aluminosilicate GME using *N,N*-dimethyl-3,5-dimethylpiperidinium (SDA3 in Table 1) and Na<sup>+</sup> cations in the synthesis gel. Since we focus on the directing role of Al, we exclude from this study any synthesis report containing inorganic cations.

From the resulting selection, a table was generated gathering basic synthesis parameters (such as Si/Al, water/Si, and the presence of fluoride in the synthesis) that were grouped by OSDA. Finally, only records involving the synthesis of different zeolites as silica and aluminosilicate were kept (see Table S1). Seven OSDAs were identified to fit those criteria. The names and the structures of these OSDAs are given in Table 1 along with the zeolite phases that are obtained under pure silica and aluminosilicate conditions. The corresponding references are indicated in the Supporting Information (Table S1).

**2.2. Force Field Simulation Details.** zeoT<sub>sda</sub> software employs the General Utility Lattice Program (GULP)<sup>46</sup> to generate a combination of Monte Carlo and lattice energy minimization techniques in order to find the lowest conformational energy of OSDAs inside zeolite micropores. In the simulations, Lennard-Jones potentials were used to describe the non-bonded two-body interactions, not only between different OSDA molecules but also within all Si, Al, and O atoms in the zeolite with a cut-off radius of 12 Å. The incorporation of long-range interactions was tackled through the Ewald summation method. The electrostatic charges of the OSDAs as well as Si(OH)<sub>4</sub>, Al(OH)<sub>3</sub>, and H<sub>2</sub>O were taken from a charge equilibration approach.<sup>47</sup> As in our previous work,<sup>42</sup> the approximation of zero overall charge for the OSDA was considered for pure silica zeolites, while for the aluminosilicate cases, the OSDAs were considered with their charge distribution corresponding to the overall cationic

charge, usually +1, except in the case of SDA7 (+2). The charges of zeolite atoms were, on the one hand,  $q(\text{Si}) = 2.1$  and  $q(\text{O}) = -1.05$  for the central SiO<sub>4</sub> tetrahedra in Si-(O<sub>4</sub>)-(SiO<sub>3/2</sub>)<sub>4</sub> units, giving an overall zero charge, and on the other hand  $q(\text{Al}) = 1.575$  and  $q(\text{O}) = -1.16875$  for the central AlO<sub>4</sub> tetrahedra in Al-(O<sub>4</sub>)-(SiO<sub>3/2</sub>)<sub>4</sub> units, giving an overall -1 charge, as obtained from the force field for silica, aluminosilicate, and silicoaluminophosphate zeolites by Bushuev and Sastre (BS).<sup>48</sup> The potential parameters of the OSDA atoms are taken from Oie et al.<sup>49</sup> The location of OSDAs and—for synthesis in fluoride media—fluoride anions inside the zeolite is determined using zeoT<sub>sda</sub>.<sup>42</sup> The software works in a fully automated way and is able to find the optimum loading of OSDAs in the zeolite micropores with the CIF of zeolite and the XYZ coordinates of the OSDA as the only input required. An approximate 5% failure has so far been experienced due mainly to difficult cases related to extremely tight-fitting zeo-OSDA pairs or highly connected zeolite micropores containing a large number of similar energetically equivalent locations. Hence, visual inspection is always recommended in order to refine possible errors. In the present study, only SDA7-ITH was incorrectly predicted by zeoT<sub>sda</sub>. In particular, the self-assembling (two molecules per cage) of SDA4 in RTH<sup>50</sup> was predicted by zeoT<sub>sda</sub>. Also, the cavity in which fluoride is located, in the case of silica in fluoride media, was correctly predicted by zeoT<sub>sda</sub> (except for ITH), although covalent Si-F bonds in small (except D4R) cavities cannot be predicted by this force field. The framework Al atoms were incorporated into the aluminosilicate zeolite models using zeoTAl software,<sup>51</sup> which generated in each case 100 random Al configurations for a given Al content, of which only the most energetically favorable was selected. The Al content was selected as that which compensates the positive charges of the optimum loading of OSDAs obtained from the zeoT<sub>sda</sub>

## Scheme 1. Synthesis Reactions of Aluminosilicate Zeolites



calculation for the corresponding pure silica zeolite. Hence, since all aluminosilicates are synthesized without fluoride, the positive charge of OSDAs is compensated exclusively by Al.

From the final geometries obtained by  $\text{zeoT}_{\text{sda}}$ , an energy decomposition was made for pure silica zeolites. For aluminosilicate phases and pure silica zeolites under fluoride media, the geometry optimization was also done by periodic DFT calculations, which are explained in detail in Section S5, to compare the results obtained by both computational methods.

**2.3. Synthesis Energy for Pure Silica and Aluminosilicate Zeolites.** A new equation that allows us to compare the stabilities of zeolites with different Si/Al ratios has been derived based on the following concept. If the synthesis of two different zeolites can be written in terms of the same reactants (as in Scheme 1), the energies of the products can be directly compared since they should have equal overall chemical compositions.

In Scheme 1, two zeolites are obtained in two reactions with the same reactants. A given zeolite ( $\text{zeo}_1$ ) is obtained (with Si/Al =  $m_1/p_1$ ) using an OSDA through condensation of Si and Al monomers, giving water as a product, but also another zeolite ( $\text{zeo}_2$ ) with different Si/Al can be obtained, giving Si and Al reactant monomers in excess ( $m_3$  and  $p_3$ ), but also another zeolite ( $\text{zeo}_2$ ) as well as OSDA. Since both reactions have the same reactants, the stability of the products can be directly compared. A more detailed analysis (see the Supporting Information, Section S3) gives the following equation that quantifies the stability, from the synthesis reaction, of a given  $\text{zeo-OSDA}$  pair.

$$E_{\text{zeo-OSDA}}^{\text{syn}} = E_{\text{zeo-OSDA}} + 2 \cdot E_{\text{H}_2\text{O}} - p/(m+p) \cdot (E_{\text{SDAOH}} + E_{\text{Al(OH)}_3}) - m/(m+p) \cdot E_{\text{Si(OH)}_4} \quad (3)$$

where  $E_{\text{zeo-OSDA}}^{\text{syn}}$  represents the total energy of the zeolite synthesis reaction,  $E_{\text{zeo-OSDA}}$  is the total energy of the pure silica (as in eqs 1 and 2) or aluminosilicate  $\text{zeo-OSDA}$  pair,  $E_{\text{SDAOH}}$  represents the energy of the OSDA molecule neutralized with a hydroxide, and “ $m$ ” and “ $p$ ” are the number of Si and Al atoms in the framework, respectively. The energies of  $\text{H}_2\text{O}$ ,  $\text{Si(OH)}_4$ , and  $\text{Al(OH)}_3$  (Tables S5 and S6) are included in eq 3 due to their energetic contribution to the oligomerization and ring closure reactions during the synthesis of zeolite.

$E_{\text{syn}}$  can be regarded as an enthalpy of reaction when considering silicon and aluminum hydroxides as sources of Si and Al. In that sense, some of the synthesis seem to be exothermic (negative values of  $E_{\text{syn}}$ ), while others seem to be endothermic (positive values of  $E_{\text{syn}}$ ). From the different possibilities considered, that with lowest enthalpy will be our prediction, regardless of the fact that the value is positive or negative. Exothermic reactions will in principle require less activation energy and will be more favorable, but also endothermic reactions are perfectly possible since the hydrothermal synthesis conditions require high pressure and temperatures in the range of 130–180 °C.

The pure silica and aluminosilicate zeolite phase obtained by each OSDA can be predicted according to the  $E_{\text{zeo-OSDA}}^{\text{syn}}$  values for all the competing zeolites and taking the lowest as the most stable. The results for the comparison of aluminosilicate zeolite-OSDA stability considering force field and DFT calculations are given in detail in Tables S6 and S9, respectively. The main results are included in Tables 2 and 3.

**Table 2.** “Synthesis Energies” of Pure Silica Phases under Fluoride and Hydroxide Media Calculated by Force Field Simulations, as from eq 3<sup>a</sup>

OSDA	Zeo	No of SiO <sub>2</sub>	Total Energy Si/F (eV/SiO <sub>2</sub> )	E(syn) Si/F (eV/SiO <sub>2</sub> )
SDA1	BEA	64	-40.800	-0.036
	CHA	36	-40.870	-0.015
	DDR	120	-40.662	-0.026
	DOH	34	-40.659	-0.040
	MTW	56	-40.691	-0.045
SDA2	SGT	64	-40.755	0.009
	AEI	48	-40.764	0.040
SDA3	SFF	64	-40.710	0.015
	AEI	48	-40.934	-0.060
SDA4	CHA	36	-40.929	-0.055
	MTW	56	-40.722	-0.068
SDA5	ITW	24	-40.883	-0.362
	RTH	32	-40.826	-0.290
SDA6	RTH	32	-40.771	-0.314
	STW	60	-40.794	-0.331
	FER	36	-40.897	-0.299
SDA7	ITW	24	-40.911	-0.340
	TON	48	-40.689	-0.159
	EUO	112	-40.895	0.249
SDA7	ITH	56	-40.977	0.167
	MRE	96	-40.807	0.065

OSDA	Zeo	No of SiO <sub>2</sub>	Total Energy Si/OH (eV/SiO <sub>2</sub> )	E(syn) Si/OH (eV/SiO <sub>2</sub> )
SDA2	AEI	48	-40.397	0.600
	SFF	64	-40.472	0.398
SDA3	AEI	48	-40.524	0.544
	CHA	36	-40.512	0.556
SDA7	MTW	56	-40.532	0.206
	EUO	112	-40.545	0.933
	ITH	56	-40.533	0.945
	MRE	96	-40.573	0.494

<sup>a</sup>The predicted (lowest energy) zeolite phase indicated in colors; green indicates a correct prediction, while red indicates a false prediction.

**2.4. Total Energy Decomposition for Pure Silica Zeolites.** A detailed energy decomposition analysis was employed considering the various energy contributions to the total energy of the  $\text{zeo-OSDA}$  system for pure silica zeolites considering the hydroxide or fluoride route, depending on the synthesis (Table S1), using a similar strategy with one

**Table 3. “Synthesis Energies” of Aluminosilicate Phases Calculated by Force Field Simulations, as from eq 3<sup>a</sup>**

OSDA	Zeo	m	p	Total Energy Si/Al (eV/TO <sub>2</sub> )	E(syn) Si/Al (eV/TO <sub>2</sub> )	Si/Al
SDA1	BEA	60	4	-40.183	-0.535	15
	CHA	33	3	-40.109	-0.742	11
	DDR	116	4	-40.368	-0.327	29
	DOH	33	1	-40.395	-0.301	33
	MTW	54	2	-40.363	-0.354	27
SDA2	SGT	60	4	-40.228	-0.580	15
	AEI	44	4	-39.999	-0.683	11
SDA3	SFF	60	4	-40.135	-0.526	15
	AEI	44	4	-40.182	-0.795	11
	CHA	33	3	-40.188	-0.801	11
SDA4	MTW	54	2	-40.399	-0.382	27
	ITW	22	2	-40.053	-1.022	11
SDA5	RTH	28	4	-39.727	-1.426	7
	RTH	28	4	-39.647	-1.426	7
SDA6	STW	54	6	-39.775	-1.101	9
	FER	32	4	-39.869	-1.261	8
	ITW	22	2	-40.073	-0.994	11
SDA7	TON	46	2	-40.274	-0.490	23
	EUO	104	8	-40.262	-0.718	13
	ITH	52	4	-40.285	-0.741	13
	MRE	92	4	-40.411	-0.473	23

<sup>a</sup>The predicted (lowest energy) zeolite phases indicated in colors; green indicates a correct prediction, while red indicates a false prediction. “m” and “p” are the number of Si and Al atoms, respectively, in a unit cell.

of our recent studies.<sup>41</sup> The total energies of the zeo-SDA systems for pure silica zeolites can be calculated using the following expressions

$$E_{\text{zeo-OSDA}} = E_{\text{zeo}} + E_{\text{OSDA}}^{\text{Coul-inter}} + E_{\text{OSDA}}^{\text{vdw}} + E_{\text{OSDA}}^{\text{intra}} + E_{\text{zeo-OSDA}}^{\text{Coul-inter}} + E_{\text{zeo-OSDA}}^{\text{vdw}} \quad (1)$$

$$E_{\text{zeo-OSDA-F}} = E_{\text{zeo}} + E_{\text{OSDAF}}^{\text{Coul-inter}} + E_{\text{OSDAF}}^{\text{vdw}} + E_{\text{OSDAF}}^{\text{intra}} + E_{\text{zeo-OSDAF}}^{\text{Coul-inter}} + E_{\text{zeo-OSDA}}^{\text{vdw}} + E_{\text{zeo-F}} \quad (2)$$

Each component in eqs 1 and 2 is essential in explaining the structure directing effect of OSDAs and the stability of the final structure. All contributions are divided by the number of SiO<sub>2</sub> in the unit cell unless otherwise specified and are explained in detail in the Supporting Information (Section S2 and Tables S3 and S4). With these components of energy, it is possible to identify the driving factor for the selection of the final zeolite

phase which is calculated depending on the synthesis energies of zeolites. For the aluminosilicate case, it is not possible to calculate separately E<sub>zeo</sub> since the framework is not neutral due to the presence of aluminum, and a periodic charged system has no chemical sense. Hence, only pairing the negatively charged framework with the counteranion (such as OSDA) is possible to calculate an energy contribution. Therefore, for aluminosilicates, we will only use the total energy, E<sub>zeo-OSDA</sub>, without energy decomposition.

### 3. RESULTS AND DISCUSSION

The force field results for the energetic analysis of pure silica and aluminosilicate zeolites are shown in Tables 2 and 3, respectively. The prediction of phase selectivity is done according to the lowest E(syn) values in these tables regardless of the fact that they are positive or negative. The predicted zeolite phases for each OSDA under pure silica and aluminosilicate conditions are presented in Table 4 along with the experimental results for the sake of comparison.

Among the seven OSDA molecules employed in this work, SDA1 was certainly the one with the worst selectivity, leading to four different pure silica phases (BEA, DDR, DOH, and SGT) and two different aluminosilicate zeolites (MTW and CHA). The final product of the pure silica phase was reported to be changing from BEA, a 3-D large pore zeolite, to DDR, a 2-D zeolite with eight-ring channels, and then eventually to DOH, a clathrasil, as the water/silica ratio increases.<sup>52</sup> This is in agreement with the general rule of thumb for zeolite synthesis that higher density products are formed with higher water/silica ratios.<sup>53</sup> All of these zeolite structures were obtained as pure silica in fluoride media; thus, we included in Table 2 the results of the calculations including F<sup>-</sup> anions to compensate the charge of SDA1. Our calculations predicted BEA, DDR, DOH, and MTW as the final pure silica products in fluoride media (E<sub>zeo-OSDA</sub><sup>syn</sup> = -0.036 eV/SiO<sub>2</sub> for BEA, -0.026 eV/SiO<sub>2</sub> for DDR, -0.040 eV/SiO<sub>2</sub> for DOH, and -0.045 eV/SiO<sub>2</sub> for MTW). All of the predicted pure silica zeolite phases were in agreement with the experiments, except for MTW. Although MTW is an aluminosilicate, Wagner et al.<sup>54</sup> were able to synthesize high-silica MTW (Si/Al = 70) using SDA1. We believe that this small Al content (less than 1 Al per unit cell) could be the reason for the shortcoming of our calculation method. When Al is included in the calculations, CHA becomes the predicted zeolite phase with a “synthesis energy” (eq 3 and Table 3) of -0.741 eV/T. Although the prediction of CHA as the aluminosilicate phase is correct based on experimental results, MTW can also be synthesized as aluminosilicate with SDA1, which is not predicted from the

**Table 4. Comparison between Force Field-Calculated Pure Silica and Aluminosilicate Zeolite Phases and Experiments (See also Table S1)**

OSDA	pure silica					
	hydroxide		fluoride		aluminosilicate	
	calculated	experiments	calculated	experiments	calculated	experiments
SDA1			BEA, DOH, MTW	BEA, SGT, DDR, DOH	CHA	CHA, MTW
SDA2	SFF	SFF	SFF	SFF	AEI	AEI
SDA3	MTW	MTW	MTW	MTW	AEI, CHA	AEI, CHA
SDA4			ITW	ITW	RTH	RTH
SDA5			STW	STW	RTH	RTH
SDA6			ITW	ITW, TON	FER	FER
SDA7	MRE	MRE	MRE	ITH	ITH	EUO

calculations, albeit—as said above—this refers to a synthesis with very low Al content ( $\text{Si}/\text{Al} = 70$ ).<sup>54</sup>

The synthesis using SDA2 and SDA3 showed some similarities as the final pure silica structures for both OSDAs were one-dimensional channel zeolites, SFF for SDA2 and MTW for SDA3, in both hydroxide and fluoride media. In hydroxide media, SFF and MTW are correctly predicted as the pure silica phases for SDA2 and SDA3, respectively, due to their favorable “synthesis energies” (0.398 eV/SiO<sub>2</sub> for SDA2-SFF and 0.206 eV/SiO<sub>2</sub> for SDA3-MTW, Table 2). The short-range interactions between SDA2 and SFF are similar to those for AEI, which is the competing phase, and so the larger stability of SDA2-SFF is due to  $E_{\text{zeo}}$  and  $E_{\text{SDA}}$  terms, the latter referring to the strain of SDA2 in each zeolite (see Table S3). For SDA3-MTW, in spite of the smaller short-range stabilization,  $E_{\text{zeo-OSDA}}^{\text{vdw}}$  (−0.024 eV/SiO<sub>2</sub>, compared to −0.068 and −0.064 eV/SiO<sub>2</sub> for AEI and CHA, respectively, Table S4), the larger stability of  $E_{\text{zeo}}$  for MTW dominates and explains the overall lowest energy for SDA3-MTW in hydroxide media. When fluoride anions were considered in the calculations, the predicted pure silica phase for both SDAs remain the same (Table 2), in agreement with the experiments (Table 4).

The inclusion of Al using SDA2 leads to AEI as the computationally predicted phase ( $E_{\text{zeo-OSDA}}^{\text{syn}} = -0.682$  eV/T). This is in perfect agreement with the experimental results. We note that, even though SFF can be synthesized with SDA2 in an aluminosilicate gel composition, the final product of the synthesis was identified to be a pure silica zeolite.<sup>55</sup> Therefore, we do not include SFF in experimental aluminosilicate phases obtained using SDA2 in Table 4. For SDA3, CHA is the phase with lowest energy as aluminosilicate, in agreement with experiments. The energy difference between CHA and AEI is very small (−0.801 and −0.795 eV/T), which suggests that both phases can be synthesized, and this is in fact the experimental result (Table 4). AEI and CHA are both 3-D open framework aluminosilicate structures containing D6R units in the framework. These examples validate the structure directing effect of Al toward more open structures.<sup>56</sup>

ITW and STW are zeolite structures containing double four-ring units (D4R) which are obtained as pure silica in fluoride media when using SDA4 and SDA5, respectively. ITW is the most stable product in our calculations with  $E_{\text{zeo-OSDA}}^{\text{syn}} = -0.362$  eV/SiO<sub>2</sub> (Table 2). Although the zeo-SDAF interactions of SDA4-RTH-F are more favorable than those for ITW, the lower SDA strain and the larger zeolite stability of ITW drive the most stable phase to ITW (see Table S4). This is due to the tight packing of OSDA molecules inside the pores of RTH, with two OSDA molecules per cage, whereas in ITW, one OSDA molecule was placed in each cage. When using SDA5 in pure silica gel and fluoride media, STW shows lower calculated “synthesis energy” than RTH (−0.331 eV/SiO<sub>2</sub> for STW and −0.314 eV/SiO<sub>2</sub> for RTH). The main factor contributing to this result is the favorable OSDA-F energy for STW (0.099 eV/SiO<sub>2</sub>) compared to RTH (0.184 eV/SiO<sub>2</sub>, Table S4) due to the smaller strain of SDA5 in STW.

When using SDA4 and SDA5, if Al is incorporated in the synthesis gel, it replaces fluoride anions as the charge balancing factor of OSDAs. As a result, the phase selectivity of the synthesis shifts from D4R-containing frameworks (ITW and STW) to RTH ( $E_{\text{zeo-OSDA}}^{\text{syn}} = -1.425$  eV/T atom for both SDAs, Table 3), containing  $[4^65^4]$  and  $[4^65^86^48^4]$  rth cavities.

Using SDA6 in pure silica gel and fluoride media gives ITW (2-D zeolite with D4R units) and TON (1-D zeolite with 10-ring channels) according to the experiments (Tables 4 and S1). Our calculations in fluoride media correctly predict ITW but failed to predict TON. In the case of ITW, the largest contribution to the selectivity came from its lower  $E_{\text{zeo-OSDAF}}$  (−0.520 eV/SiO<sub>2</sub>, compared to −0.491 and −0.184 eV/SiO<sub>2</sub> for FER and TON, respectively, Table S4). When Al atoms are incorporated into the synthesis, the final product switches to FER, which is correctly predicted from the calculations (Table 3).

For SDA7, pure silica zeolite synthesis in hydroxide media correctly predicts MRE as the most stable phase. Having less favorable short-range interactions with the OSDA,  $E_{\text{z-SDA}}(\text{vdw})$  in Table S3, compared to its competitors, the synthesis of MRE is driven by its larger stability ( $E_{\text{zeo}} = -40.573$  eV/SiO<sub>2</sub>) with respect to ITH and EUO (−40.529 and −40.528 eV/SiO<sub>2</sub>, respectively). Addition of fluoride to the synthesis shifts the synthesis product from MRE, a 1-D 10 MR channeled zeolite, to ITH (3D) with D4R units, which could not be predicted by our fluoride media calculations, although MRE can also appear at low fluoride concentration and alkaline pH.<sup>57,58</sup> Inclusion of Al atoms in the synthesis with SDA7 changes the predicted final product to EUO, which is this time only predicted by the periodic DFT ( $E_{\text{zeo-OSDA}}^{\text{syn,DFT}} = -0.711$  and −0.699 eV/T for EUO and ITH, respectively, Table S8) and not by the force field calculations ( $E_{\text{zeo-OSDA}}^{\text{syn,ff}} = -0.718$  and −0.740 eV/T for EUO and ITH, respectively, Table 3). In all other cases, there is a qualitative agreement between both methods. Since the aluminosilicate gel does not contain fluoride anions, the stabilizing role of fluoride-D4Rs in ITH is not present, and this contributes to EUO being the phase obtained.

When all the results for the aluminosilicate zeolites are examined in detail, it is observed that competing phases with lower Si/Al have a lower synthesis energy. This is in fact an expected outcome since the energy of incorporating Al into the framework is more favorable than the energy of Si incorporation into the framework. Zeolites are in fact, naturally, aluminosilicates. This effect becomes more pronounced especially when the topology of the zeolite allows occlusion of more OSDA molecules into the micropores, leading to an increased amount of Al atoms in the framework (lower Si/Al). Finally, we wanted to investigate how the synthesis energies would be affected if two zeolites would have the same Si/Al. Thus, in Table S12, we compared the synthesis energies of ITW and TON with the same Si/Al = 23 using SDA6. In this case, ITW is the preferred phase due to the favorable zeolite–SDA interactions. Therefore, when Si/Al is the same for two competing phases, the SDA packing drives the synthesis instead of the Al incorporation energy.

## 4. CONCLUSIONS

Overall, both computational methods we used in this work gave in general correct predictions for the most stable zeolite phases obtained under pure silica and aluminosilicate conditions according to their  $E_{\text{syn}}$  values, and the energetic analysis was able to elucidate the structure directing effects of OSDA and Al atoms in the framework. A few cases remain with wrong predictions from the calculations, and this indicates the direction for future work. Nevertheless, the fact that the lowest  $E_{\text{syn}}$  value (hence lowest energy) indicates the experimentally synthesized phase shows that this is an excellent

descriptor. We suggest that this descriptor can be employed in future work by other groups. The presence of defects, effect of water/silica, temperature, and kinetic factors are still not properly accounted in our methods. Within the aluminosilicate competing phases, that containing the lower Si/Al tends to be more stable. This follows from the relative enthalpies of incorporating aluminum vs silicon, as well as from the ability of the competing phases to occlude a large number of OSDA molecules per T-atom (hence more Al and lower Si/Al), maximizing the short-range zeo-OSDA energetic stabilization.

## ■ ASSOCIATED CONTENT

### SI Supporting Information

The Supporting Information is available free of charge at <https://pubs.acs.org/doi/10.1021/acs.jpcc.3c01567>.

Details of synthesis; energetic analysis of pure silica zeolites; energetic analysis of aluminosilicate zeolites; energetic analysis of pure silica and aluminosilicate zeolites with/without fluoride using force fields and periodic DFT; and fluoride locations (PDF)

CAR files of OSDA molecules used in this study with neutral and cationic charge (ZIP)

CIF files with coordinates of all final geometries of zeo-OSDA and zeo-OSDA-F systems calculated in this study (ZIP)

## ■ AUTHOR INFORMATION

### Corresponding Author

German Sastre – Instituto de Tecnología Química UPV/CSIC, Universidad Politécnica de Valencia, 46022 Valencia, Spain; [orcid.org/0000-0003-0496-6331](https://orcid.org/0000-0003-0496-6331); Phone: +34963879445; Email: [gsastre@itq.upv.es](mailto:gsastre@itq.upv.es)

### Authors

Omer F. Altundal – Instituto de Tecnología Química UPV/CSIC, Universidad Politécnica de Valencia, 46022 Valencia, Spain

Santiago Leon – Instituto de Tecnología Química UPV/CSIC, Universidad Politécnica de Valencia, 46022 Valencia, Spain

Complete contact information is available at: <https://pubs.acs.org/10.1021/acs.jpcc.3c01567>

### Author Contributions

The manuscript was written through contributions of all authors. All authors have given approval to the final version of the manuscript.

### Notes

The authors declare no competing financial interest.

## ■ ACKNOWLEDGMENTS

We thank GVA for PROMETEO/2021/077 project as well as ASIC-UPV and SGAI-CSIC for the use of computational facilities. S.L. thanks MICINN for predoctoral grant BES-2017-081245 corresponding to project SEV-2016-0683-17-2.

## ■ REFERENCES

- (1) Bodart, P.; Nagy, J. B.; Debras, G.; Gabelica, Z.; Jacobs, P. A. Aluminum Siting in Mordenite and Dealumination Mechanism. *J. Phys. Chem.* **1986**, *90*, 5183–5190.
- (2) Bohinc, R.; Hoszowska, J.; Dousse, J.-C.; Blachucki, W.; Zeeshan, F.; Kayser, Y.; Nachtegaal, M.; Pinar, A. B.; van Bokhoven, J. A. Distribution of Aluminum over Different T-Sites in

Ferrierite Zeolites Studied with Aluminum Valence to Core X-Ray Emission Spectroscopy. *Phys. Chem. Chem. Phys.* **2017**, *19*, 29271–29277.

- (3) Dědeček, J.; Sklenak, S.; Li, C.; Wichterlová, B.; Gábová, V.; Brus, J.; Sierka, M.; Sauer, J. Effect of Al–Si–Al and Al–Si–Si–Al Pairs in the ZSM-5 Zeolite Framework on the 27Al NMR Spectra. A Combined High-Resolution 27Al NMR and DFT/MM Study. *J. Phys. Chem. C* **2009**, *113*, 1447–1458.

- (4) Ahn, S. H.; Wang, Q.; Wang, Y.; Chu, Y.; Deng, F.; Hong, S. B. Identifying Crystallographically Different Si–OH–Al Brønsted Acid Sites in LTA Zeolites. *Angew. Chem., Int. Ed.* **2022**, *61*, No. e202203603.

- (5) Sklenak, S.; Dědeček, J.; Li, C.; Wichterlová, B.; Gábová, V.; Sierka, M.; Sauer, J. Aluminum Siting in Silicon-Rich Zeolite Frameworks: A Combined High-Resolution 27Al NMR Spectroscopy and Quantum Mechanics/Molecular Mechanics Study of ZSM-5. *Angew. Chem., Int. Ed.* **2007**, *46*, 7286–7289.

- (6) Li, C.; Vidal-Moya, A.; Miguel, P. J.; Dedecek, J.; Boronat, M.; Corma, A. Selective Introduction of Acid Sites in Different Confined Positions in ZSM-5 and Its Catalytic Implications. *ACS Catal.* **2018**, *8*, 7688–7697.

- (7) Ghorbanpour, A.; Rimer, J. D.; Grabow, L. C. Computational Assessment of the Dominant Factors Governing the Mechanism of Methanol Dehydration over H-ZSM-5 with Heterogeneous Aluminum Distribution. *ACS Catal.* **2016**, *6*, 2287–2298.

- (8) Biligetu, T.; Wang, Y.; Nishitoba, T.; Otomo, R.; Park, S.; Mochizuki, H.; Kondo, J. N.; Tatsumi, T.; Yokoi, T. Al distribution and catalytic performance of ZSM-5 zeolites synthesized with various alcohols. *J. Catal.* **2017**, *353*, 1–10.

- (9) Chu, W.; Liu, X.; Yang, Z.; Nakata, H.; Tan, X.; Liu, X.; Xu, L.; Guo, P.; Li, X.; Zhu, X. Constrained Al Sites in FER-Type Zeolites. *Chin. J. Catal.* **2021**, *42*, 2078–2087.

- (10) Vjunov, A.; Fulton, J. L.; Huthwelker, T.; Pin, S.; Mei, D.; Schenter, G. K.; Govind, N.; Camaioni, D. M.; Hu, J. Z.; Lercher, J. A. Quantitatively Probing the Al Distribution in Zeolites. *J. Am. Chem. Soc.* **2014**, *136*, 8296–8306.

- (11) Perea, D. E.; Arslan, I.; Liu, J.; Ristanović, Z.; Kovarik, L.; Arey, B. W.; Lercher, J. A.; Bare, S. R.; Weckhuysen, B. M. Determining the Location and Nearest Neighbours of Aluminium in Zeolites with Atom Probe Tomography. *Nat. Commun.* **2015**, *6*, 7589.

- (12) Jones, A. J.; Carr, R. T.; Zones, S. I.; Iglesia, E. Acid Strength and Solvation in Catalysis by MFI Zeolites and Effects of the Identity, Concentration and Location of Framework Heteroatoms. *J. Catal.* **2014**, *312*, 58–68.

- (13) Berkson, Z. J.; Hsieh, M.-F.; Smeets, S.; Gajan, D.; Lund, A.; Lesage, A.; Xie, D.; Zones, S. I.; McCusker, L. B.; Baerlocher, C.; et al. Preferential Siting of Aluminum Heteroatoms in the Zeolite Catalyst Al-SSZ-70. *Angew. Chem., Int. Ed.* **2019**, *58*, 6255–6259.

- (14) Opalka, S. M.; Zhu, T. Influence of the Si/Al Ratio and Al Distribution on the H-ZSM-5 Lattice and Brønsted Acid Site Characteristics. *Microporous Mesoporous Mater.* **2016**, *222*, 256–270.
- (15) Yokoi, T.; Mochizuki, H.; Namba, S.; Kondo, J. N.; Tatsumi, T. Control of the Al Distribution in the Framework of ZSM-5 Zeolite and Its Evaluation by Solid-State NMR Technique and Catalytic Properties. *J. Phys. Chem. C* **2015**, *119*, 15303–15315.

- (16) Losch, P.; Joshi, H. R.; Vozniuk, O.; Grünert, A.; Ochoa-Hernández, C.; Jabraoui, H.; Badawi, M.; Schmidt, W. Proton Mobility, Intrinsic Acid Strength, and Acid Site Location in Zeolites Revealed by Varying Temperature Infrared Spectroscopy and Density Functional Theory Studies. *J. Am. Chem. Soc.* **2018**, *140*, 17790–17799.

- (17) Lu, B.; Kanai, T.; Oumi, Y.; Sano, T. Aluminum Distribution in High-Silica Mordenite. *J. Porous Mater.* **2007**, *14*, 89–96.

- (18) Ghorbanpour, A.; Rimer, J. D.; Grabow, L. C. Periodic, VdW-Corrected Density Functional Theory Investigation of the Effect of Al Siting in H-ZSM-5 on Chemisorption Properties and Site-Specific Acidity. *Catal. Commun.* **2014**, *52*, 98–102.

- (19) Dědeček, J.; Sobalík, Z.; Wichterlová, B. Siting and Distribution of Framework Aluminium Atoms in Silicon-Rich Zeolites and Impact on Catalysis. *Catal. Rev.* **2012**, *54*, 135–223.
- (20) Gallego, E. M.; Li, C.; Paris, C.; Martín, N.; Martínez-Triguero, J.; Boronat, M.; Moliner, M.; Corma, A. Making Nanosized CHA Zeolites with Controlled Al Distribution for Optimizing Methanol-to-Olefin Performance. *Chem.—Eur. J.* **2018**, *24*, 14631–14635.
- (21) Jeffroy, M.; Nieto-Draghi, C.; Boutin, A. New Molecular Simulation Method To Determine Both Aluminum and Cation Location in Cationic Zeolites. *Chem. Mater.* **2017**, *29*, 513–523.
- (22) Shantz, D. F.; Fild, C.; Koller, H.; Lobo, R. F. Guest–Host Interactions in As-Made Al-ZSM-12: Implications for the Synthesis of Zeolite Catalysts. *J. Phys. Chem. B* **1999**, *103*, 10858–10865.
- (23) Shantz, D. F.; Lobo, R. F.; Fild, C.; Koller, H. Controlling the Distribution of Framework Aluminum in High-Silica Zeolites. In *Studies in Surface Science and Catalysis*; Corma, A., Melo, F. V., Mendioroz, S., Fierro, J. L. G., Eds.; *12th International Congress on Catalysis*; Elsevier, 2000; Vol. 130, pp 845–850.
- (24) Shantz, D. F.; Lobo, R. F. Guest-Host Interactions in Zeolites as Studied by NMR Spectroscopy: Implications in Synthesis, Catalysis and Separations. *Top. Catal.* **1999**, *9*, 1–11.
- (25) Li, S.; Gounder, R.; Debellis, A.; Müller, I. B.; Prasad, S.; Moini, A.; Schneider, W. F. Influence of the N,N,N-Trimethyl-1-Adamantyl Ammonium Structure-Directing Agent on Al Substitution in SSZ-13 Zeolite. *J. Phys. Chem. C* **2019**, *123*, 17454–17458.
- (26) Sabater, M. J.; Sastre, G. A Computational Study on the Templating Ability of the Trispyrrolidinium Cation in the Synthesis of ZSM-18 Zeolite. *Chem. Mater.* **2001**, *13*, 4520–4526.
- (27) Lok, B. M.; Cannan, T. R.; Messina, C. A. The Role of Organic Molecules in Molecular Sieve Synthesis. *Zeolites* **1983**, *3*, 282–291.
- (28) Gies, H.; Marker, B. The Structure-Controlling Role of Organic Templates for the Synthesis of Porosils in the Systems SiO<sub>2</sub>/Template/H<sub>2</sub>O. *Zeolites* **1992**, *12*, 42–49.
- (29) Burton, A. W.; Zones, S. I.; Elomari, S. The Chemistry of Phase Selectivity in the Synthesis of High-Silica Zeolites. *Curr. Opin. Colloid Interface Sci.* **2005**, *10*, 211–219.
- (30) Davis, M. E.; Lobo, R. F. Zeolite and Molecular Sieve Synthesis. *Chem. Mater.* **1992**, *4*, 756–768.
- (31) Muraoka, K.; Chaikittisilp, W.; Yanaba, Y.; Yoshikawa, T.; Okubo, T. Directing Aluminum Atoms into Energetically Favorable Tetrahedral Sites in a Zeolite Framework by Using Organic Structure-Directing Agents. *Angew. Chem., Int. Ed.* **2018**, *57*, 3742–3746.
- (32) Lewis, D. W.; Richard A Catlow, C.; Thomas, J. M. Application of Computer Modelling to the Mechanisms of Synthesis of Microporous Catalytic Materials. *Faraday Discuss.* **1997**, *106*, 451–471.
- (33) Turrina, A.; Garcia, R.; Cox, P. A.; Casci, J. L.; Wright, P. A. Retrosynthetic Co-Templating Method for the Preparation of Silicoaluminophosphate Molecular Sieves. *Chem. Mater.* **2016**, *28*, 4998–5012.
- (34) Sastre, G.; Cantin, A.; Diaz-Cabañas, M. J.; Corma, A. Searching Organic Structure Directing Agents for the Synthesis of Specific Zeolitic Structures: An Experimentally Tested Computational Study. *Chem. Mater.* **2005**, *17*, 545–552.
- (35) Jo, D.; Hong, S. B. Charge Distribution and Conformational Stability Effects of Organic Structure-Directing Agents on Zeolite Synthesis. *Chem. Commun.* **2018**, *54*, 487–490.
- (36) Moliner, M.; Rey, F.; Corma, A. Towards the Rational Design of Efficient Organic Structure-Directing Agents for Zeolite Synthesis. *Angew. Chem., Int. Ed.* **2013**, *52*, 13880–13889.
- (37) Di Iorio, J. R.; Li, S.; Jones, C. B.; Nimlos, C. T.; Wang, Y.; Kunkes, E.; Vattipalli, V.; Prasad, S.; Moini, A.; Schneider, W. F.; et al. Cooperative and Competitive Occlusion of Organic and Inorganic Structure-Directing Agents within Chabazite Zeolites Influences Their Aluminum Arrangement. *J. Am. Chem. Soc.* **2020**, *142*, 4807–4819.
- (38) Burton, A. W.; Zones, S. I. Chapter 5 - Organic Molecules in Zeolite Synthesis: Their Preparation and Structure-Directing Effects. In *Studies in Surface Science and Catalysis*; Čejka, J., van Bekkum, H., Corma, A., Schüth, F., Eds.; *Introduction to Zeolite Science and Practice*; Elsevier, 2007; Vol. 168, pp 137–179.
- (39) Li, J.; Corma, A.; Yu, J. Synthesis of New Zeolite Structures. *Chem. Soc. Rev.* **2015**, *44*, 7112–7127.
- (40) Dusselier, M.; Davis, M. E. Small-Pore Zeolites: Synthesis and Catalysis. *Chem. Rev.* **2018**, *118*, 5265–5329.
- (41) Leon, S.; Sastre, G. Zeolite Phase Selectivity Using the Same Organic Structure-Directing Agent in Fluoride and Hydroxide Media. *J. Phys. Chem. C* **2022**, *126*, 2078–2087.
- (42) Gálvez-Llompert, M.; Cantin, A.; Rey, F.; Sastre, G. Computational Screening of Structure Directing Agents for the Synthesis of Zeolites. A Simplified Model. *Z. Kristallogr.—Cryst. Mater.* **2019**, *234*, 451–460.
- (43) Schwalbe-Koda, D.; Kwon, S.; Paris, C.; Bello-Jurado, E.; Jensen, Z.; Olivetti, E.; Willhammar, T.; Corma, A.; Román-Leshkov, Y.; Moliner, M.; et al. A Priori Control of Zeolite Phase Competition and Intergrowth with High-Throughput Simulations. *Science* **2021**, *374*, 308–315.
- (44) CAS SciFinder. <https://scifinder-n.cas.org/> (accessed Nov 18, 2022).
- (45) Dusselier, M.; Kang, J. H.; Xie, D.; Davis, M. E. CIT-9: A Fault-Free Gmelinite Zeolite. *Angew. Chem., Int. Ed.* **2017**, *56*, 13475–13478.
- (46) Gale, J. D. GULP: A Computer Program for the Symmetry-Adapted Simulation of Solids. *J. Chem. Soc., Faraday Trans.* **1997**, *93*, 629–637.
- (47) Rappe, A. K.; Casewit, C. J.; Colwell, K. S.; Goddard, W. A. I.; Skiff, W. M. UFF, a Full Periodic Table Force Field for Molecular Mechanics and Molecular Dynamics Simulations. *J. Am. Chem. Soc.* **1992**, *114*, 10024–10035.
- (48) Bushuev, Y. G.; Sastre, G. Atomistic Simulations of Structural Defects and Water Occluded in SSZ-74 Zeolite. *J. Phys. Chem. C* **2009**, *113*, 10877–10886.
- (49) Oie, T.; Maggiora, G. M.; Christoffersen, R. E.; Duchamp, D. J. Development of a Flexible Intra- and Intermolecular Empirical Potential Function for Large Molecular Systems. *Int. J. Quantum Chem.* **1981**, *20*, 1–47.
- (50) Schmidt, J. E.; Deimund, M. A.; Xie, D.; Davis, M. E. Synthesis of RTH-Type Zeolites Using a Diverse Library of Imidazolium Cations. *Chem. Mater.* **2015**, *27*, 3756–3762.
- (51) Lemishko, T.; Valencia, S.; Rey, F.; Jiménez-Ruiz, M.; Sastre, G. Inelastic Neutron Scattering Study on the Location of Brønsted Acid Sites in High Silica LTA Zeolite. *J. Phys. Chem. C* **2016**, *120*, 24904–24909.
- (52) Zones, S. I.; Burton, A. W.; Lee, G. S.; Olmstead, M. M. A Study of Piperidinium Structure-Directing Agents in the Synthesis of Silica Molecular Sieves under Fluoride-Based Conditions. *J. Am. Chem. Soc.* **2007**, *129*, 9066–9079.
- (53) Cambor, M. A.; Villaescusa, L. A.; Díaz-Cabañas, M. J. Synthesis of All-Silica and High-Silica Molecular Sieves in Fluoride Media. *Top. Catal.* **1999**, *9*, 59–76.
- (54) Wagner, P.; Nakagawa, Y.; Lee, G. S.; Davis, M. E.; Elomari, S.; Medrud, R. C.; Zones, S. I. Guest/Host Relationships in the Synthesis of the Novel Cage-Based Zeolites SSZ-35, SSZ-36, and SSZ-39. *J. Am. Chem. Soc.* **2000**, *122*, 263–273.
- (55) Wagner, P.; Zones, S. I.; Davis, M. E.; Medrud, R. C. SSZ-35 and SSZ-44: Two Related Zeolites Containing Pores Circumscribed by Ten- and Eighteen-Membered Rings. *Angew. Chem., Int. Ed.* **1999**, *38*, 1269–1272.
- (56) Burton, A. W.; Lee, G. S.; Zones, S. I. Phase Selectivity in the Syntheses of Cage-Based Zeolite Structures: An Investigation of Thermodynamic Interactions between Zeolite Hosts and Structure Directing Agents by Molecular Modeling. *Microporous Mesoporous Mater.* **2006**, *90*, 129–144.
- (57) Bats, N.; Rouleau, L.; Paillaud, J.-L.; Caillet, P.; Mathieu, Y.; Lacombe, S. Recent Developments in the Use of Hexamethonium Salts as Structure Directing Agents in Zeolite Synthesis. In *Studies in Surface Science and Catalysis*; van Steen, E., Claeys, I. M., Callanan, L.



H., Eds.; *Recent Advances in the Science and Technology of Zeolites and Related Materials*; Elsevier, 2004; Vol. 154, pp 283–288.

(58) Liu, X.; Ravon, U.; Tuel, A. Synthesis of All-Silica Zeolites from Highly Concentrated Gels Containing Hexamethonium Cations. *Microporous Mesoporous Mater.* **2012**, *156*, 257–261.

## Recommended by ACS

### Does Water Enable Porosity in Aluminosilicate Zeolites? Porous Frameworks versus Dense Minerals

Karel Asselman, Eric Breynaert, *et al.*

MARCH 24, 2023  
CRYSTAL GROWTH & DESIGN

READ 

### Interzeolite Transformation of Borosilicate MWW to Metallosilicate BEA-Type Zeolites: Separated Kinetics of Structural Transformation and Metal Substitution

Sungjoon Kweon, Min Bum Park, *et al.*

JUNE 08, 2023  
CHEMISTRY OF MATERIALS

READ 

### Superior Thermostability of Poly-Silicic Acid Analogues of Zeolite Composite/Secondary Building Units: A Theoretical Investigation

Xin Liu, Changgong Meng, *et al.*

FEBRUARY 02, 2023  
THE JOURNAL OF PHYSICAL CHEMISTRY C

READ 

### Hydrothermal Synthesis and Catalytic Assessment of High-Silica (B,Fe)-beta Zeolites

Alessia Marino, Girolamo Giordano, *et al.*

MARCH 07, 2023  
CRYSTAL GROWTH & DESIGN

READ 

Get More Suggestions >